Thermochimica Acta, 64 (1983) 83–106
Elsevier Science Publishers B.V., Amsterdam – Printed in The Netherlands

THERMAL AND MÖSSBAUER STUDIES OF IRON-CONTAINING HYDROUS SILICATES. IV. AMESITE

K.J.D. MACKENZIE and M.E. BOWDEN
Chemistry Division, DSIR, Private Bag, Petone (New Zealand)
(Received 15 October 1982)

ABSTRACT

X-Ray diffraction, thermal analysis, infrared and Mössbauer studies of the thermal reactions of amesites from Saranovskoye, U.S.S.R., and Chester, U.S.A., show that amesites appear to dehydroxylate in at least two stages. The first stage, at about 550–800°C, results in the collapse of some regions to an almost cubic close-packed structure which probably retains a cation configuration similar to the reactant, and is responsible for the broad, transitory X-ray reflections previously reported. The early-stage reaction is also complicated by the conversion of some 7 Å amesite regions to a chloritic 14 Å structure which coexists with the 7 Å structure and collapsed regions to about 900°C. At 900–1000°C the 7 Å structure decomposes with the immediate formation of a cubic spinel. The previously-formed collapsed phase also disappears at this stage, the products being crystalline spinel, sapphirine and forsterite. Similar reactions occur under reducing conditions. Thermally-induced changes in the iron sites are discussed, and the possible reaction mechanism compared with those of structurally-related minerals.

INTRODUCTION

Amesite is one of a group of four minerals which are chemically related to the chlorites but have structural similarities with the kaolinite–serpentine minerals, being composed of alternate tetrahedral and trioctahedral layers. The resulting basal spacing is similar to that of kaolinite (7 Å), which has led to the suggestion [1] that this group should be called septechlorites, to distinguish them from the normal chlorites, which possess a 14 Å basal spacing.

The mineral was first described by Shepard (in ref. 2), who named it amesin (or amesine) in honour of James Ames, the proprietor of the Chester emery mines, Massachusetts, U.S.A., from which the type mineral had come. On establishing the validity of the mineral as a new species, Shepard changed the name to its present form, amesite.

The chemical formula of ideal amesite is $(Mg_4Al_2)(Si_2Al_2)O_{10}(OH)_8$, containing no iron, but showing extensive substitution of Al for both Si in the tetrahedral layers and Mg in the octahedral. In this respect, it can be

0040-6031/83/$03.00

considered as being derived from serpentine ($Mg_6Si_4O_{10}(OH)_8$) by partial replacement of Mg and Si by Al. In natural amesites, however, substitution of ferrous iron for octahedral Mg can also occur. Thus, the structural formula of the type material was deduced by Brindley et al. [3] from an earlier chemical analysis to be $(Mg_{3.0}Al_{2.12}Fe^{2+}_{0.82})(Si_2Al_2)O_{10}(OH)_8$. Furthermore, the possible presence of ferric iron must also be considered, since the Mössbauer spectrum of an amesite from a different location [4] seems to suggest the occurrence of small amounts of Fe^{3+} in both tetrahedral and octahedral sites, in addition to octahedral Fe^{2+}. This result is all the more interesting since it was obtained using a specimen which previously had been the subject of a crystallographic study [5], but for which no chemical analysis has been reported.

The thermal decomposition sequence of the Chester amesite has been partially determined by Brindley et al. [3], who reported it to decompose at ~ 600°C, forming a transitory phase, tentatively identified as fayalite (Fe_2SiO_4), at 800°C. A spinel is said to be formed above 900°C [3]. In a more recent study of a different amesite, Steinfink and Brunton [5] suggest that the X-ray lines attributed by Brindley et al. [3] to fayalite are diffuse reflections caused by stacking disorder induced in the crystal by the heat treatment.

The present study was undertaken to shed further light on the structure and thermal reaction sequence of the two previously studied amesites, by carrying out the decomposition under carefully controlled oxidising and reducing conditions, and studying the reaction products using a number of analytical techniques.

EXPERIMENTAL

Material

Two well-characterised amesites were used in this study. The first, designated A1, was from the Saranovskoye Chromite Deposit, Northern Urals, U.S.S.R., and came from specimen 103312 of the mineral collection of the Smithsonian Institution, Washington. Good quality, pale violet-to-colourless crystals, which were hand-picked from the groundmass, gave a very intense amesite X-ray powder pattern, the only other detectable feature being a very small 14 Å reflection. Although this sample was previously used in the X-ray study of Steinfink and Brunton [5] and in the Mössbauer study of Taylor et al. [4], no chemical analysis has previously been published; an atomic absorption analysis was therefore carried out (Table 1). Semi-quantitative arc spectral analysis showed the major trace elements in this material to be Cr and Ni (> 500 ppm each), Cu (500 ppm), Ti (400 ppm), Zn and Pb (250 ppm each).

The second amesite, designated A2, was from the Emery Mine, Chester, Massachusetts, U.S.A., and came from specimen 80715 of the mineral collection, Smithsonian Institution, Washington. This sample, from which very pale green crystals were picked, was the one studied by Brindley et al. [3]. The reported chemical analysis is shown in Table 1. The major trace impurity in this material was found by semi-quantitative arc spectral analysis to be Ti (2000 ppm), with smaller amounts of Ni and Co (150 ppm each) also present. X-Ray powder diffraction showed a sharp amesite pattern, with some weak additional reflections, notably at 14.03 Å and 2.82 Å, as previously reported by Brindley et al. [3], and attributed by them to a chlorite impurity. Most of the present work was carried out on the whole sample, on which no attempt had been made to remove the chlorite by the thermal and

TABLE 1

Chemical analyses and unit cell contents of amesites, calculated on the basis of 10 O + 8 (OH)

Component		Values (%) for					
		Saranovskoye [a] sample 1		Chester [b] sample 2		Ideal amesite 3	
SiO_2		21.42		20.95			
TiO_2		0.26					
Al_2O_3		34.06		35.21			
Fe_2O_3		0.63					
FeO		0.95		8.28			
MgO		28.66		22.88			
CaO		0.08		0.58			
Na_2O		0.38					
K_2O		0.05					
MnO		< 0.01		Tr			
H_2O		13.50		12.25			
Total		99.99		101.15			
Unit cell contents							
Si	T_d	2.02	4.0	2.01	4.0	2.0	4.0
Al		1.98		1.99		2.0	
Al		1.82		2.0		2.0	
Fe^{3+}	O_h	1.14	6.10	–	5.94	–	6.0
Fe^{2+}		0.08		0.66		–	
Mg		4.08		3.28		4.0	
OH		8		8		8	
O		10		10		10	

[a] Column 1. Specimen 103312, Saranovskoye Chromite deposit, N. Urals. Analyst, A.D. Cody.

[b] Column 2. Specimen 80715, Chester, Mass. Analyst, F.V. Shannon (1921) [6].

acid treatments described by Brindley et al. [3], but a few additional X-ray and Mössbauer experiments were made on amesites freed from chlorite by the Brindley method.

Table 1 shows the unit cell contents calculated from the chemical analyses for the two amesites, both of which are in good agreement with the structural formula for ideal amesite, which is included in Table 1 for comparison.

Methods

Samples of each amesite were heated in platinum-lined ceramic boats, both in static air and a flowing H_2/N_2 mixture (5% H_2, 95% N_2; 0.6 l min^{-1}) at various temperatures determined with reference to the DTA curves obtained under the same atmospheres with a Stone model 202 thermal analyser at a heating rate of 10°C min^{-1}. After each incremental heating, the samples were examined by X-ray powder diffraction and IR spectroscopy. The Mössbauer spectra were obtained at room temperature using an Elscint AME 40 spectrometer with a Co/Rh source. All isomer shifts are quoted with respect to soft iron. Weight-loss curves were determined using a Stanton TG770 thermobalance in flowing gas atmospheres (0.04 l min^{-1}) at a heating rate of 10°C min^{-1}, the evolved gas from some of these experiments being analysed by an Extranuclear quadrupole mass spectrometer.

RESULTS AND DISCUSSION

(a) Thermal analysis

The DTA and TG curves for the two amesites are shown in Fig. 1. In addition to a low-temperature endotherm at ~ 100°C corresponding to the loss of loosely-held moisture, both amesites show at least three higher-temperature endotherms in all atmospheres. The temperatures and intensities of these endotherms are atmosphere-dependent, in some cases appearing to be split. The final endotherm is in some cases followed by a small exotherm corresponding to the formation of crystalline product phases. A similar three-endotherm feature was previously reported in the DTA trace of Chester amesite in air by Nelson and Roy [7], who suggest that the first endotherm (at ~ 700°C) is typical of a 14 Å chlorite, whereas the second endotherm is characteristic of 7 Å serpentine; these results are taken to indicate that this amesite is a mixture of two chlorite polymorphs, but no explanation is offered for the third endotherm at ~ 900°C. Present X-ray diffraction results [section (b)] indicate that the final endotherm/exotherm feature is associated with the breakdown of the amesite structure to form crystalline products at ~ 800–1000°C. Clearly, amesite has considerably

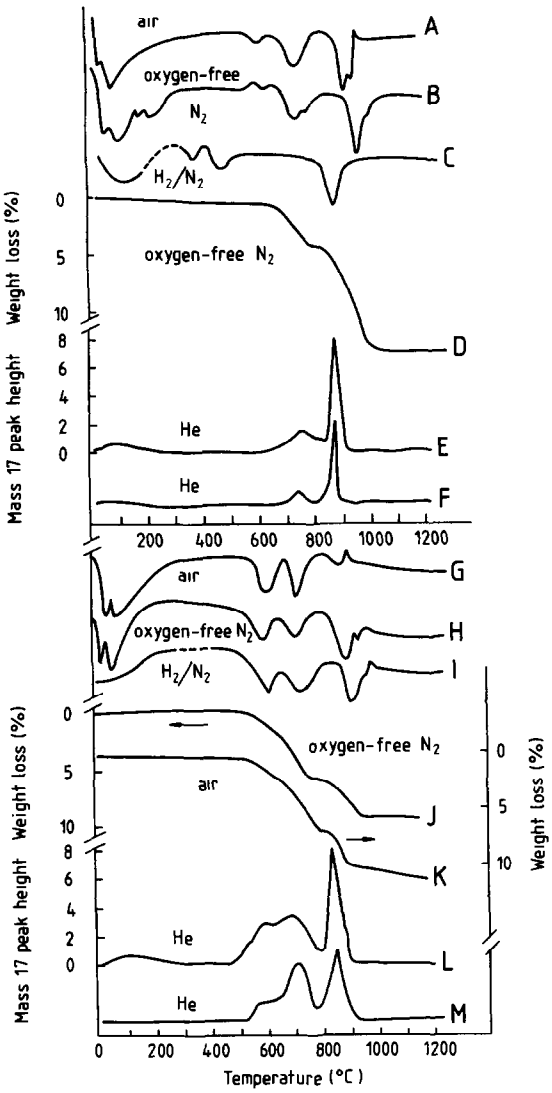

Fig. 1. Thermal analysis curves of amesites. Curves A–F, sample A1 (Saranovskoye); curves G–M, sample A2 (Chester). Heating rate for DTA (curves A–C, G–I) and TG (curves D, J and K), 10°C min^{-1}. Dashed portion of DTA curves C and I indicates region where background curve was subtracted to eliminate noise due to adsorption of H_2 by the platinel thermocouples. Heating rate of EGA (curves E and L) and DTG (curves F and M), 15°C min^{-1}; carrier gas, He. Only mass 17 (water) presented; no other evolved species detected.

greater thermal stability than related serpentine varieties, which undergo endothermic dehydroxylation at ~ 635°C [8].

In considering whether one or both of the lower-temperature endotherms might be explained in terms of a 14 Å component, account must be taken of two possible alternatives: (i) that the 14 Å component is a physically-mixed

impurity, as suggested by Brindley et al. [3] on the basis of their ability to remove this phase by thermal and acid treatments without destroying the amesite, or (ii) the 14 Å and related reflections arise from regular interstratification of chlorite-like and amesite-like regions as has been shown to occur in a Cornish daphnite [9]. As a further possible complication, Nelson and Roy [7] have demonstrated the development of 14 Å spacings in amesite and related 7 Å minerals by prolonged heating at 590°C; this process was observed in Chester amesite (A2) irrespective of the presence or absence of the physically-mixed chlorite contaminant [7].

Although the temperatures of the present endotherms at ~ 600° and ~ 750°C agree reasonably well with the decomposition temperatures of typical chlorites, in which the brucite layer decomposes at ~ 600°C with the loss of 12 hydroxyls per formula unit, the mica layer losing its 4 hydroxyls per formula unit at ~ 800°C [8], these endotherms are probably not associated with the destruction of a discrete 14 Å impurity phase, for the following reasons:

(i) The intensities of these endotherms appear too large to be accounted for by the relatively small 14 Å chlorite concentrations indicated by X-ray diffraction [section (b)].

(ii) Comparison of the TG weight losses associated with these endotherms (Fig. 1, curves D and J) with theoretical weight losses calcualted for mixtures of ideal amesite and chlorite of assumed formula $Si_2Al_4Mg_4O_{10}(OH)_8$ and $[Mg_4Al_2(OH)_{12}][(Si_6Al_2)Mg_6O_{20}(OH)_4]$, respectively, confirms that the concentration of admixed chlorite must be very small in A1 but slightly greater in A2. The theoretical total weight losses for the decomposition of these chlorites (~ 0.8% from A1 and ~ 1.5% from A2) are too small to account for the total weight losses associated with the lower-temperature endotherms (4.4% and 5.5% in A1 and A2, respectively).

The EGA curves (Fig. 1, curves E and L) indicate that the water removed during the lower-temperature endotherms is relatively loosely bound, evolving gradually over a 200°C temperature interval, by contrast with the final sharp water loss associated with the complete breakdown of the amesite structure. This distinction is also evident from the corresponding DTG curves (Fig. 1, curves F and M). Further, X-ray diffraction [section (b)] indicates that the lower-temperature water losses coincide with the appearance of intense new peaks which reach maximum development at ~ 800°C and disappear simultaneously with the disappearance of the amesite structure at ~ 900°C. Thus, rather than being associated with the decomposition of a discrete chlorite impurity, these endotherms and their associated weight losses appear to reflect the gradual elimination of less-tightly-bound water, resulting in a progressive collapse to a structure giving the intense new X-ray lines.

The role of the 14 Å phase in these thermal events is less clear; the small amount initially present must decompose at some stage, as will any 14 Å

regions which may form during subsequent heating [7]. Although the thermal effects of chlorite impurity are probably not very significant, it is possible that the interstratified 14 Å regions which develop later might be associated with the centres from which the less-tightly-bound water is lost, but the present results provide little direct evidence on this point.

(b) X-Ray diffraction

The 14 Å phase in unheated amesite

The appearance in amesite X-ray traces of small peaks corresponding to 001 reflections where l is odd indicates a 14 Å layer structure coexisting with the 7 Å amesite structure which contains only the even l basal reflections. Gruner [10] explained this in terms of the presence of one 14 Å chlorite unit interlayered between each 10–16 amesite units, resulting in a large *c*-axis superlattice which restrains the curvature of the 7 Å units. The later conclusions of Brindley et al. [3] regarding a mechanically-mixed impurity have already been mentioned, as has the observation that 14 Å structures can be thermally generated in amesite [7]. The more recent crystallographic studies of amesite [5,11] have not addressed the question of 14 Å structures.

If, as suggested by Brindley et al. [3], the chlorite is a discrete phase, aspects of its constitution can be deduced from careful measurement of its 001 and 060 spacings [12]. The former provides information on the degree of Al-for-Si substitution while the latter can be used to calculate the *b*-parameter of the cell, which is related to the degree of substitution of octahedral Mg by Fe^{2+} [12].

Although determinations of the *b*-parameter from the 060 spacing are not satisfactory in mixtures of 7 Å and 14 Å phases, since this reflection is common to both phases, in the present case, measurements made using a silicon standard give an estimate of the limiting values of *b*, and probably do better than this, since even at very slow scan speeds, no splitting of the 060 reflection was observed, suggesting that in the present 7 Å and 14 Å phases, these reflections coincide closely.

Assuming the 14 Å phase is a discrete trioctahedral chlorite with equal octahedral and tetrahedral Al substitution, these measurements suggest formulae of $(Mg_{4.27}Fe^{2+}_{0.03}Al_{1.7})(Si_{2.30}Al_{1.70})O_{10}(OH)_8$ and $(Mg_{3.4}Fe^{2+}_{0.4}Al_{2.2})(Si_{1.8}Al_{2.2})O_{10}(OH)_8$ for the chlorites from A1 and A2, respectively. These chlorite compositions are similar to those reported for sheridanites (ref. 13, analyses 12 and 13) rather than the more iron-rich corundophilite (ref. 13, analysis 10) which is reported as the accessory chlorite mineral with Al. This suggests that the iron contents of both A1 and A2 are associated with the 7 Å rather than the 14 Å phase.

Experiments with A1 and A2 which had been purified by the method of Brindley et al. [3] show that while this treatment significantly reduces the

intensities of all the 001 reflections associated with the 14 Å phase (particularly the 003), these reflections are not entirely eliminated, possibly because of the appearance of Nelson and Roy's more stable interstratified 14 Å phase [7] during thermal treatment. Thus, the distinction between interstratified and physically-mixed 14 Å phases is difficult, since the treatment used to remove one may simultaneously generate the other.

Effect of heat treatment

The phases detectable by X-ray diffraction are shown schematically as a function of temperature in Fig. 2.

On heating in air, both amesites undergo small expansions in the 002 spacing up to about 500°C; A1 increases from 6.97 Å to 7.08 Å and A2 from 6.97 Å to 7.02 Å, but the 14 Å spacing in both amesites is unchanged. At

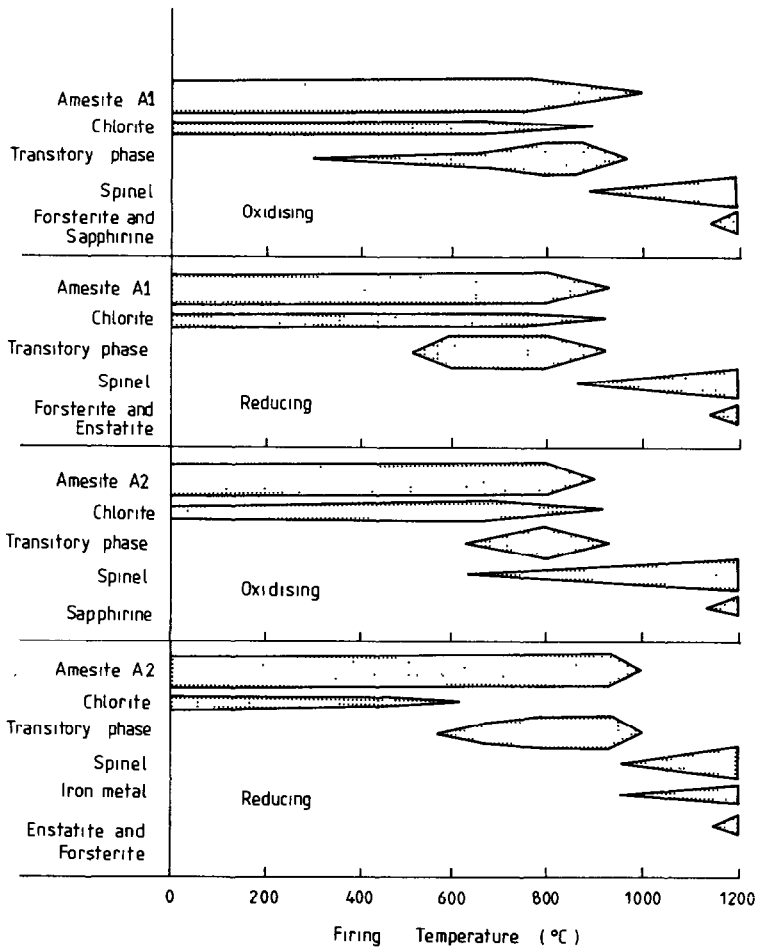

Fig. 2. Schematic representation of the phases formed from amesites as a function of temperature under oxidising and reducing conditions.

500–600°C, broad, intense X-ray peaks occur in both amesites, confirming previous findings [3,5] (Fig. 3, curves C and D).

At about 600–700°C, the 14 Å spacing begins to lose intensity, eventually disappearing at 800–900°C, at which temperature the amesite peaks and the intense transitory peaks also disappear, the latter rather abruptly. At about 800–900°C, spinel ($MgAl_2O_4$) appears, with a trace of corundum (Al_2O_3) also present in A2. The presence of a less-crystalline material (probably siliceous) is suggested in both A1 and A2 by a broad hump in the X-ray trace at about 20–40°2θ; by 1200°C this feature has been replaced by crystalline silicates [sapphirine ($Mg_{3.5}Al_9Si_{1.5}O_{20}$) in A2 and forsterite

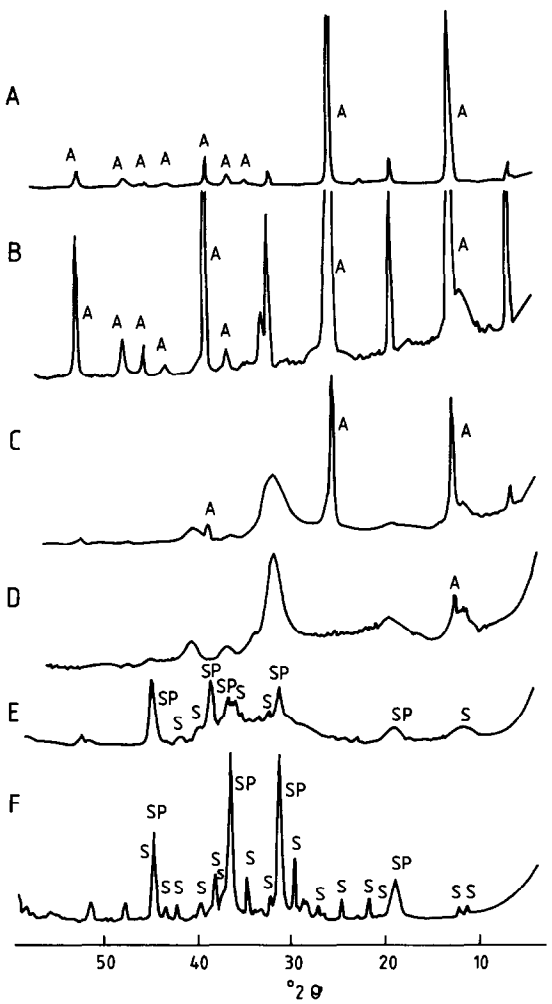

Fig. 3. Typical X-ray traces of heated and unheated amesite A2 (Chester), showing development of transitory peaks. A, Unheated; B, 550°C (higher sensitivity); C, 750°C; D, "purified" sample, 800°C; E, 1000°C; F, 1200°C. A = amesite, S = sapphirine, Sp = spinel.

(Mg_2SiO_4) with a small amount of sapphirine in A1]. No iron-rich phases are observed, but Mössbauer spectroscopy [section (d)] suggests that the iron is located exclusively in the sapphirine phase.

The formation of spinel, sapphirine, corundum and olivine from amesite heated in air has interesting geochemical implications, since similar suites of minerals are typical of emery deposits (as at Cortlandt, New York, where the sapphirine is thought to result from reaction of spinel with corundum and quartz [14]). Sapphirine is also known to form by high-temperature reaction between other minerals of this suite (e.g., alumina/enstatite solid solutions with sillimanite [15]) but previous considerations of the geochemistry of the emery deposits have not taken account of the role of thermal alteration of amesite and related hydrous minerals, or the possible reversibility of these reactions under hydrothermal conditions.

The thermal behaviour of amesites under reducing conditions is very similar to that under oxidising conditions, with the appearance of new broad peaks at 500–600°C and their disappearance at ~ 900°C. The high-temperature phases in both amesites are again predominantly spinel, with evidence of less crystalline material and again a trace of corundum in A2. By 1200°C, mixtures of forsterite and enstatite ($MgSiO_3$) have recrystallized, these phases being typical high-temperature products of serpentines, in which forsterite forms first, followed by enstatite at higher temperatures [16]. The formation of poorly crystalline material, rather than crystalline forsterite, immediately after dehydroxylation is typical of serpentines with high surface area such as the fibrous form chrysotile [16], and is also consistent with the absence of significant recrystallization exotherms in the present DTA traces.

The origin of the broad transitory X-ray peaks

The new broad peaks which appear at the onset of water loss (Fig. 3, curve B) grow with increasing temperature under both oxidising and reducing conditions (Fig. 3, curve C). "Purified" amesite behaves similarly and with carefully controlled heating, gives an X-ray trace virtually free of the original 7 Å and 14 Å phases (Fig. 3, curve D) [although more typically the new peaks disappear simultaneously with the final collapse of the amesite structure and the appearance of new phases (Fig. 3, curve E)]. Thermal analysis suggests that the transitory peaks represent a state intermediate between fully hydrated and fully dehydrated amesite, which also co-exists with the 7 Å and 14 Å structures. The *d*-values of the new peaks also bear strong similarities to those of the cubic product phases. Two possibilities therefore arise: (i) the structure giving rise to these peaks is amesite with a stacking sequence modified slightly by partial dehydration [5], or (ii) the structure is based on a cubic close-packed oxygen framework resulting from the collapse of some regions of the amesite, i.e. a precursor product phase.

To investigate these two possibilities, the *d*-values in "purified" amesite heated at 800°C were measured using Si powder as a standard (Table 2,

column a). For comparison, the *d*-values for amesite were calculated from the orthohexagonal cell parameters given by Hall and Bailey [11] (Table 2, column b). Agreement is reasonable, provided the major peak observed at $d = 2.84$ Å is indexed as the 005 reflection as previously suggested [5]. However, the new structure contains fewer peaks than would be expected for a true 7 Å or 14 Å structure, and the absence of all other 001 (1 odd) peaks is not consistent with an amesite only slightly modified by dehydration.

The *d*-values of possible cubic close-packed phases based on spinel and sapphirine structures were computed using a programme of Evans et al. [17] which refines the cell constants to take account of the observed *d*-values and then calculates a new set of *d*-values from the revised cell constants. A reasonable fit to several observed peaks was given by a spinel having a cell constant (7.962 Å) not too different from that of $MgAl_2O_4$ (8.033 Å), but not all the observed peaks could be accounted for in terms of the simple cubic structure (Table 2, column d). On the other hand, a satisfactory fit to all the observed peaks is given by a monoclinic structure similar to that of sapphirine (Table 2, column c), by making only small changes to the published cell constants [18]. Although the crystal structure of sapphirine is based on cubic close-packed oxygens, it differs from spinel in consisting of octahedral

TABLE 2

Observed and calculated X-ray data for the transitory peaks of heated amesite.

Purified amesite, [a] observed (a)	Amesite, [b] computed (b)		Sapphirine, [c] computed (c)		Cubic spinal cell, [d] computed (d)	
	hkl	d_{calc} (Å)	*hkl*	d_{calc} (Å)	*hkl*	d_{calc} (Å)
d_{obs} (Å)						
7.41 (b)	002	6.286 [e]	110	7.676		
4.55	020	4.604	200	4.522	111	4.597
2.838 [e]	005	2.812 [f]	122	2.833	220	2.815
2.660	201	2.611	013	2.649		
2.470	202	2.483	$\bar{2}52$	2.467 [e]	311	2.401 [e]
2.237	203	2.308	$\bar{1}14$	2.251	222	2.298

[a] Column (a). Observed spacings from "purified" amesite, heated in air at 800°C, Si powder standard.

[b] Column (b). Computed for amesite, orthohexagonal cell. $a = 5.319$ Å, $b = 9.208$ Å, $c = 14.060$ Å, $\alpha = 90.01°$, $\beta = 90.27°$, $\gamma = 89.96°$, space group $C1$ (ref. 11).

[c] Column (c). Computed for sapphirine-like monoclinic cell. $a = 11.187$ Å, $b = 14.518$ Å, $c = 9.999$ Å, $\beta = 126.06°$, space group $P2_1/a$ (ref. 18).

[d] Column (d). Computed for cubic spinel cell, $a = 7.962$ Å.

[e] Major peak.

[f] Not allowed in 7 Å structure.

"walls" (arrangements of octahedra intermediate between those of a chain and a sheet), connected by corner-sharing tetrahedral chains [18]. The cations in this unusual structure are extensively ordered, to compromise between nearest neighbour electroneutrality requirements and intercation repulsion effects; since extensive cation ordering is also a feature of amesites [11] [section (c)], the formation of a transitory structure with elements of a sapphirine-like sub-lattice would preserve structural continuity in partially dehydrated amesite. Thus, the present results suggest that the new peaks result from a rather more drastic collapse of the lattice layers than the stacking disorder suggested by Steinfink and Brunton [5], although structural elements of the reactant are maintained even in these regions. The co-existence of 7 Å (and 14 Å) structure with new collapsed regions is consistent with the thermal analysis results that some of the water in amesite is more loosely bound, but the nature of these less stable regions and the reasons for their instability are not immediately obvious.

(c) Infrared spectroscopy

Typical infrared spectra of unheated and heated samples are shown in Fig. 4. The unheated spectra of A1 and A2 are identical (Fig. 4, curves A and B), contrary to the spectra of these two amesites published by Serna et al. [19], whose Saranovskoye (A1) spectrum shows fewer, broader bands, consistent with a more random tetrahedral Al-for-Si substitution than found in Chester amesite (A2). The present spectra indicate the existence of both amesites in equally well-ordered forms, and support the conclusions of Hall and Bailey [11], who after re-examining previous X-ray data for Saranovskoye amesite found evidence of cation ordering in this material as well as in Chester and other amesites. The anomalous IR spectrum found by Serna et al. for A1 is most probably an artifact of their sampling procedure.

The hydroxyl stretching bands at 3620 and 3420 cm^{-1} in unheated amesite (Fig. 4, curves A and B) have been assigned respectively to the inner and outer hydroxyl groups of the octahedral sheets [19], hydrogen-bonded to adjacent oxygens in the terahedral sheets. The presence of only one outer hydroxyl band has been presented as evidence for ordered Al-for-Si substitution in Chester amesite [19] since in ordered samples, the tetrahedral oxygens are all coordinated to similar Al–Si pairs, and thus all the outer hydroxyl bands are of similar frequency. On this basis, the present spectra of A1 and A2 are both of characteristically ordered type. The origin of the shoulders in A1 and A2 at 3340 and 3250 cm^{-1} (Fig. 4, curves A and B) is unclear, but may be associated with 14 Å phases, since chlorites containing a high proportion of Al in dioctahedral sites show an additional hydroxyl band at ~ 3365 cm^{-1} [20]. By comparison with the spectra of related serpentine minerals [21], the strong bands at 980–985 cm^{-1} and that at 930 cm^{-1} have been identified as Si–O stretching frequencies, the latter being typical of

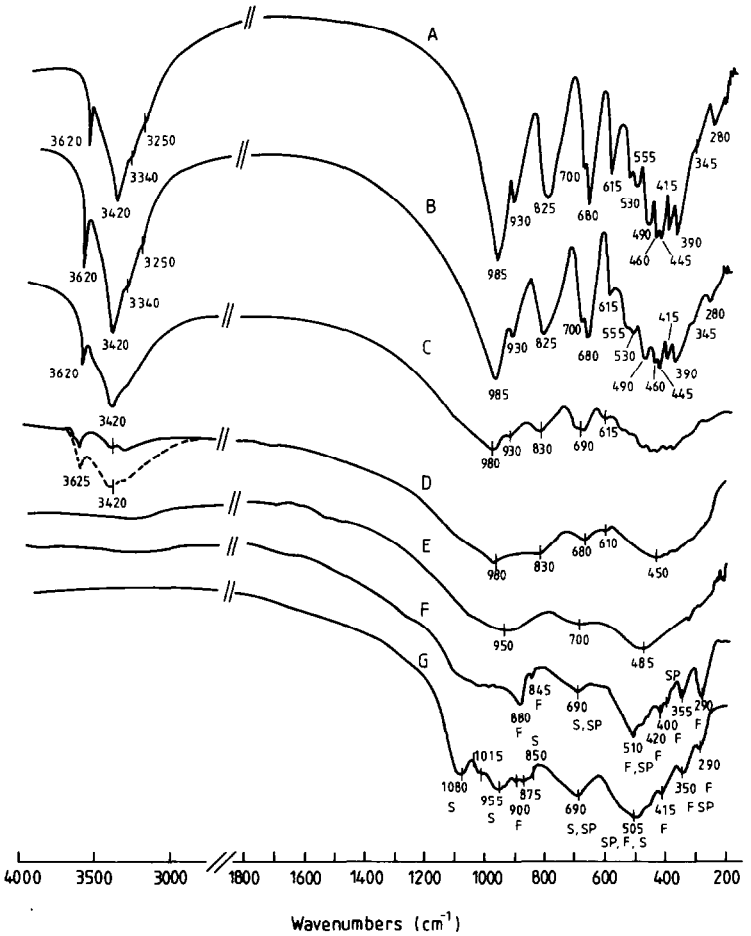

Fig. 4. Typical infrared spectra of heated and unheated amesites. A, Sample A1, Saranovskoye, unheated; B, sample A2 (Chester), unheated; C, 650°C; D, 800°C, dashed hydroxyl spectrum A1, full line A2; E, 1000°C; F, sample A1, 1200°C; G, sample A2, 1200°C. S = sapphirine, Sp = spinel, F = forsterite.

Al-rich synthetic serpentines [19]. The appearance of two Si–O bands in this region has been cited as further evidence for cation ordering [21], since a regular 1 : 1 Al-for-Si substitution changes the symmetry of the tetrahedral sheets to C_{3v}, for which two IR-active bands are expected between 900 and 1200 cm^{-1} [21]. Bands in the region 765–825 cm^{-1} assigned to AlO_4 vibrations are said also to be sensitive to tetrahedral cation ordering [19], since disordered amesites contain both isolated and condensed AlO_4 units, and show two bands at about this frequency (765 and 820 cm^{-1}) [19]. On this basis, the single prominent band at 825 cm^{-1} in the present amesites confirms their ordered nature. However, the additional band noted at ~ 765 cm^{-1} in disordered amesites [19] may merely indicate a substantial amount

of 14 Å chlorite, which has a distinctive band at 750–760 cm^{-1} [20]. The bands at 680 cm^{-1} (hydroxyl libration) and 615 cm^{-1} are common to serpentines and 14 Å chlorites with high tetrahedral Al content [20]. The remaining bands have been assigned as given: 500–555 cm^{-1}, AlO_6 vibration [21]; 460–490 cm^{-1}, combination of AlO_6 and SiO stretch [21]; ~ 450 cm^{-1}, Si–O bending mode [21]; 390–415 cm^{-1}, OH bending modes [21].

Effect of heating on IR spectra

On heating, the amesite spectral features remain recognisable to almost 800°C, although over the temperature range of the first significant water loss (~ 650–800°C), the spectra broaden and some detail is lost (Fig. 4, curve C). The persistence of the peaks at 930 and ~ 825 cm^{-1} and both the inner and outer hydroxyl peaks suggests that no change in cation ordering has occurred, and neither do the spectra show any new features which can be related to the new X-ray peaks observed in this temperature range.

Between 800–1000°C, further detail is lost (Fig. 4, curve D), but elements of the original structure persist, including the Si–O band at 980 cm^{-1}, the AlO_4 band at 830 cm^{-1} a weak hydroxyl band at 680 cm^{-1} and the AlO_6–SiO_4 frequencies at ~ 450 cm^{-1}. Although the 930 cm^{-1} peak, which is indicative of cation ordering, has disappeared by 1000°C, the inner and outer hydroxyl peaks, although weak, can still be distinguished (Fig. 4, curve D).

Above 1000°C, a very broad, 3-peak spectrum occurs (Fig. 4, curve E), with bands at ~ 950, 700 and 458 cm^{-1} and a shoulder at ~ 330 cm^{-1}; these bands are generally similar to those of cubic $MgAl_2O_4$ (720, 530 and 300 cm^{-1}) [22]. The Si–O band at ~ 950 cm^{-1} does not correspond with amorphous silicas, which typically absorb at 1080, 800 and 470 cm^{-1} (ref. 20, p. 368), but is more comparable with a cubic β-phase silicate or so-called "modified spinel" which contains Si_2O_7 groups [23]. The IR spectrum of β-Mg_2SiO_4 is unknown, but the closely-related β-Co_2SiO_4 has bands at 910, 801, 473 and 343 cm^{-1}, in addition to the symmetric Si–O–Si stretching frequency characteristic of Si_2O_7, at ~ 686 cm^{-1} [23]. Thus, spectrum E in Fig. 4 is consistent with that of a mixture of cubic $MgAl_2O_4$ and a "modified spinel" form of silicate, which at 1200°C in air gives rise to the IR bands of sapphirine [24] and forsterite (ref. 20, p. 289), superimposed on the broader spinel bands (Fig. 4, curves F and G). The forsterite spectrum is stronger in A1 (Fig. 1, curve F) whereas the sapphirine spectrum is stronger in A2 (Fig. 1, curve G), confirming the X-ray results [section (b)]. The IR spectra of both amesites fired in reducing conditions are similar to those in air, but the temperatures at which some of the spectral changes occur vary slightly with atmosphere.

Thus, the IR spectra indicate a persistence of cation ordering and thermal stability of amesite to high temperatures. Progressive thermal dehydration results in the formation of cubic aluminate and silicate phases, with no IR evidence of intermediate stages involving amorphous silica.

(d) Mössbauer spectroscopy

The Mössbauer spectra of the unheated amesites are shown in Fig. 5. Both amesites show an intense doublet corresponding to octahedral Fe^{2+} (quadrupole splitting, QS = 2.59–2.61 mm s^{-1}, isomer shift, IS = 1.11–1.13 mm s^{-1}), with an appreciable octahedral Fe^{3+} doublet (QS = 0.57, IS = 0.35 mm s^{-1}) also present in A1 (Fig. 5). The QS values of these Fe^{2+} and Fe^{3+} doublets are similar to those reported previously for Urals amesite [4], but no evidence was found in the present A1 spectrum for the previously-reported tetrahedral Fe^{3+} doublet [4]. The marked asymmetry of the present spectra, particularly in A2, has previously been reported in platy chlorite samples prone to preferred orientation [25]; by rotating the sample-plane to make an angle of ~ 147° with the γ-ray beam, the effect of orientation-induced asymmetry is removed [25]. Although such rotation of the present

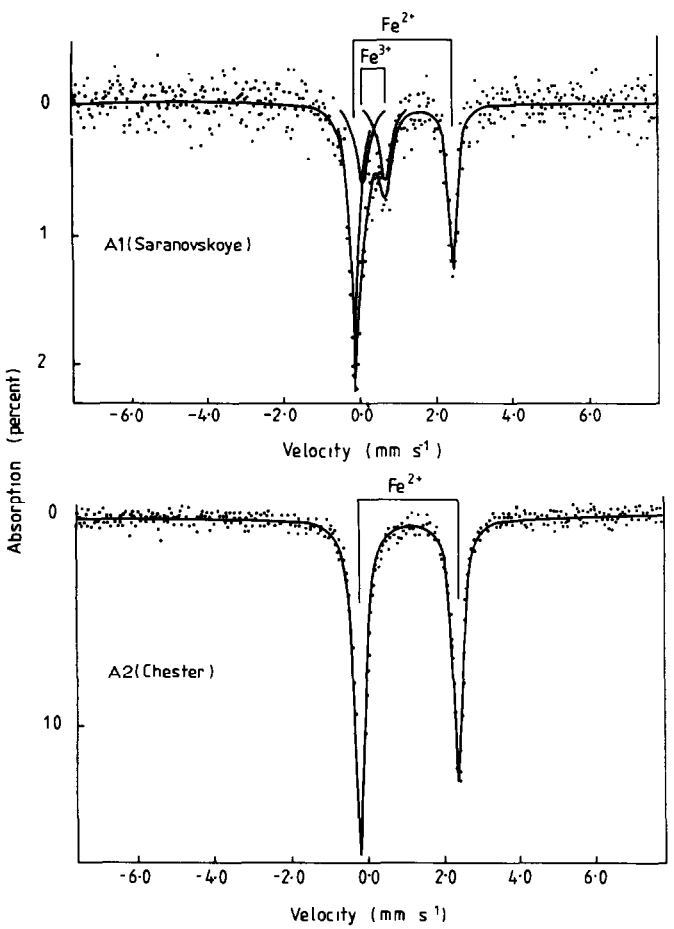

Fig. 5. Room-temperature Mössbauer spectra of unheated amesites. Source, Co/Rh.

samples eliminated the asymmetry showing it to be due to orientation effects, most of the spectra were recorded at normal incidence because of the awkward sample geometry and longer counting times associated with the rotated samples.

The Mössbauer parameters of unheated A1 and A2 are identical to those reported for the M2 sites in the serpentine minerals antigorite [26] and chrysotile [27] (QS = 2.65–2.74, IS = 1.12–1.14 mm s^{-1} for Fe^{2+}; QS = 0.75–0.80, IS = 0.34–0.43 mm s^{-1} for Fe^{3+}), and are also very similar to the parameters reported for 14 Å chlorites [25,28] (QS = 2.62–2.68, IS = 1.13–1.16 mm s^{-1} for Fe^{2+}; QS = 0.56–0.80, IS = 0.38–0.44 mm s^{-1} for Fe^{3+}). Thus, since Mössbauer spectroscopy cannot determine whether the iron in the present samples is located in the 7 Å or 14 Å impurity phase, the spectra of "purified" A1 and A2 were obtained and found to be identical to the unpurified spectra. This supports the X-ray result that the chloritic impurity material contains little iron; the following Mössbauer results therefore pertain to amesite and not its chloritic impurity.

Changes in the Mössbauer spectra of A1 and A2 on heating are shown in Figs. 6 and 7, respectively. The Mössbauer absorption of both amesites decreases to about half its original value during thermal reaction at ~ 600–800°C; this is not a serious problem in A2, in which the initial absorption is ~ 16%, but the lower-iron A1, with an initial absorption of only ~ 2% gives very poor spectra when heated at > 800°C, despite long counting times.

Changes in the relative occupancy of the various iron sites derived semi-quantitatively from the areas of the computer-fitted spectra of A1 and A2 heated in air are shown in Fig. 8. In air, the octahedral Fe^{2+} sites of both amesites are gradually oxidised at ~ 550–800°C to octahedral Fe^{3+} (QS = 1.26–1.61, IS = 0.29–0.41 mm s^{-1}). During oxidation, the QS of the original octahedral Fe^{3+} of A1 gradually increases to 0.99 mm s^{-1}, indicating increasing distortion of these sites. At the temperature of amesite structure breakdown (~ 950°C), this ferric doublet is replaced by another with parameters (QS = 0.31, IS = 0.25 mm s^{-1}) similar to those reported for tetrahedral Fe^{3+} in heated serpentine [28], but the poor quality of the A1 spectra militates against a confident assignment of this site. In A2, a second ferric doublet becomes significant at ~ 800°C, which, together with the doublet formed by oxidation of the original Fe^{2+}, forms an unusual spectrum almost identical to that obtained by Bancroft et al. for yellow sapphirine [29]. The previous identification of these two iron sites in sapphirine as four-coordinate [29] was made without the benefit of complete structural information; the parameters of the narrower doublet appear more typically octahedral and may represent sites either in the octahedral wall-building unit or in the unit between the walls [18].

The site occupancy changes in A1 and A2 heated in H_2/N_2 are shown in Fig. 9. In A1, the original octahedral Fe^{2+} sites persist to a late stage of

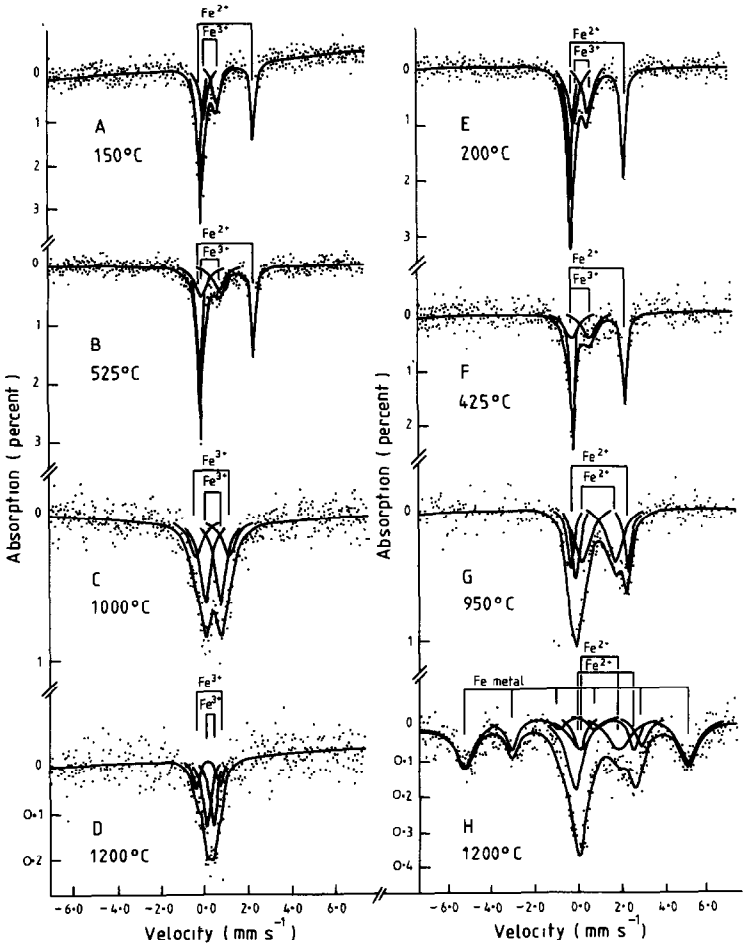

Fig. 6. Room-temperature Mössbauer spectra of heated amesite A1. Spectra A–D, air atmosphere; spectra E–H, H_2/N_2 atmosphere.

dehydration, being replaced at > 800°C by another Fe^{2+} resonance with a smaller QS, a change which is commonly taken to indicate increased site distortion (although this interpretation has been questioned for the 1 : 1 layer silicates [26]). The ferric doublet in A1 also persists to > 800°C, with a progressive increase in its QS up to ~ 650°C, indicating increased distortion, and a sudden increase in its IS just before its disappearance at ~ 800°C. The population of original Fe^{2+} sites in A2 decreases at 400–500°C, being progressively replaced by two other Fe^{2+} sites (Fig. 9). This behaviour is very similar to that reported for a low-iron 14 Å chlorite [28], in which two new Fe^{2+} resonances appeared at 750°C in an inert atmosphere; the site with the smaller QS was identified with partly dehydroxylated octahedral units such as $Fe^{2+}(O_5OH)$ or $Fe^{2+}(O_4OH\square)$ [28]. The parameters of the

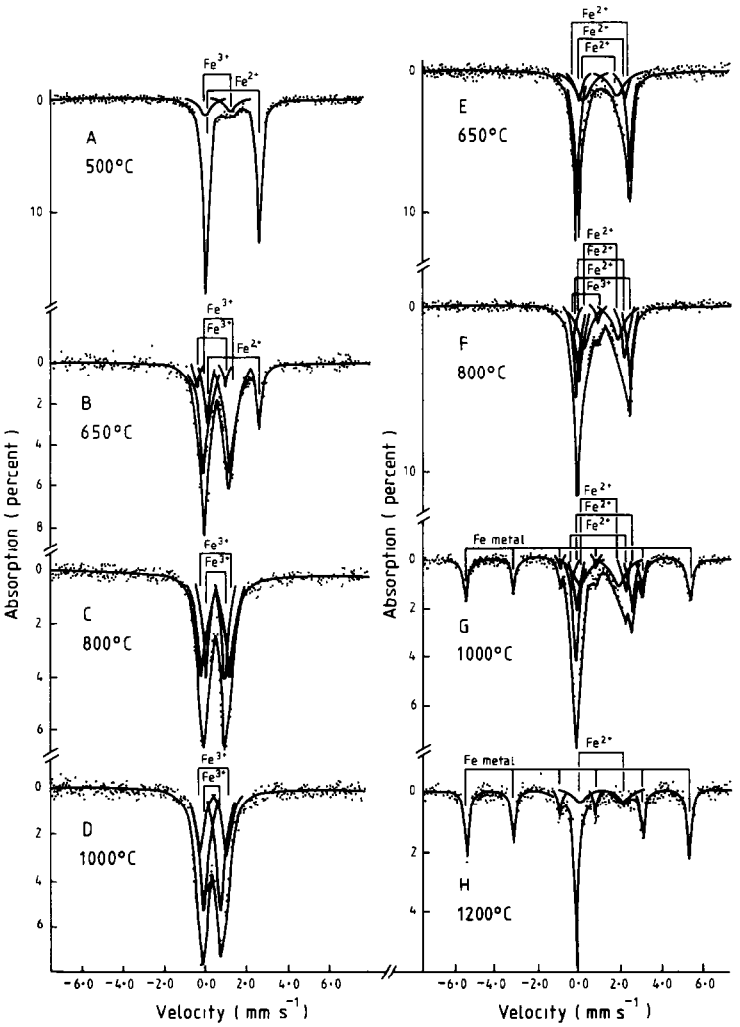

Fig. 7. Room-temperature Mössbauer spectra of heated amesite A2. Spectra A–D, air atmosphere; spectra E–H, H_2/N_2 atmosphere.

Fe^{2+} site in A2 with the smaller QS are very similar to those of the late-developing Fe^{2+} site in A1. The transitory appearance of a ferric doublet in A2 suggests that dehydroxylation is accompanied by internal oxidation (Fig. 9). Further reduction of A2 at higher temperatures produces a magnetic 6-line iron metal spectrum and an unusual sharp singlet peak with a very small IS (-0.09 to -0.10 mm s^{-1}); a similar but broader spectrum is found in A1 at 1200°C in H_2/N_2 (Fig. 6). Almost identical singlet spectra have been found in various calcium silicates reacted with iron oxides at 1300°C in air and then reduced [30], as well as in CaO, MgO and MgO and $MgAl_2O_4$ similarly treated (to be published). These systems have

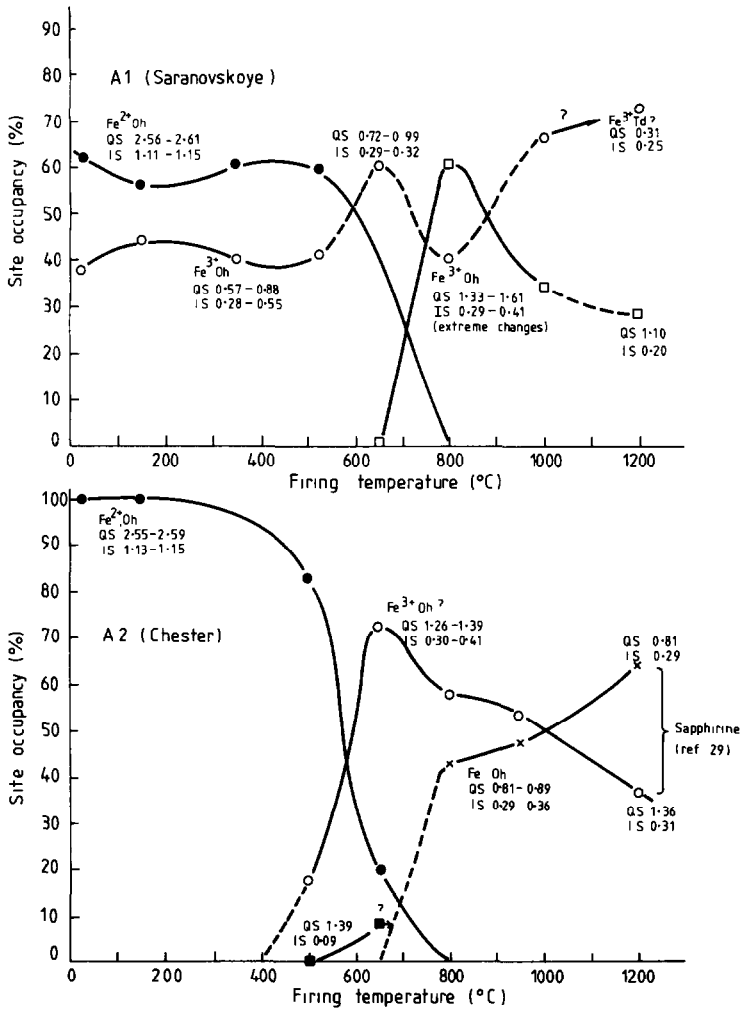

Fig. 8. Iron site occupancy changes in amesites heated in air, deduced from Mössbauer peak areas. Isomer shifts quoted with respect to natural iron. Dashed lines indicate uncertainty in site assignments due to extreme fluctuations in Mössbauer parameters.

in common a cubic oxygen structure (the entry of iron into the calcium silicate structures causes the separation of some cubic CaO). The identification of the singlet peak with a highly symmetrical cubic site is consistent with the absence of a QS; substitution of Fe^{2+} in cubic MgO is reported [31] to give a sharp singlet with an IS of ~ 0.6 mm s^{-1} (recalculated with respect to soft iron). The almost zero IS values of the present singlets are more consistent with finely dispersed superparamagnetic iron metal. Since the ferric sapphirine spectrum of oxidised A2 (Fig. 7) can be converted to the singlet spectrum by reduction at 1200°C, it appears a more likely host for the singlet sites than the cubic spinel also present.

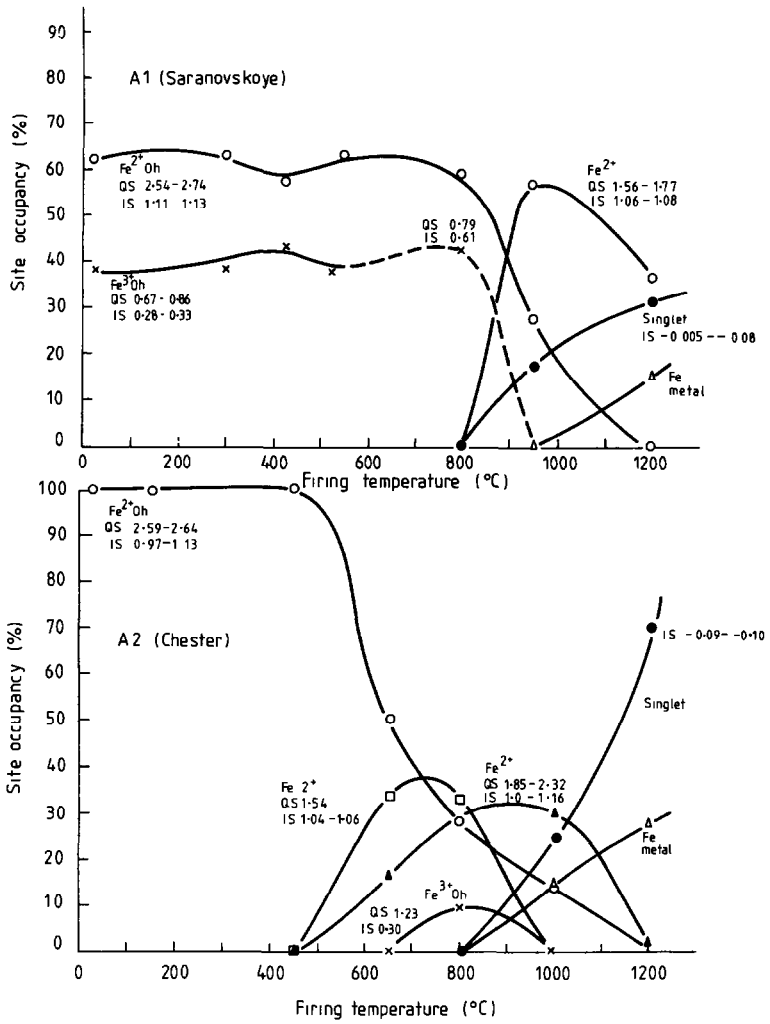

Fig. 9. Iron site occupancy changes in amesites heated in H_2/N_2, deduced from Mössbauer peak areas. Isomer shifts quoted with respect to natural iron. Dashed lines indicate uncertainty in site assignments due to extreme fluctuations in Mössbauer parameters.

(e) Mechanistic implications

Amesite appears to dehydroxylate in at least two stages; the first, at ~ 550–800°C, results in the collapse of some regions to an almost cubic close-packed structure which probably retains a cation configuration similar to the hydroxylated material, and is responsible for the broad X-ray reflections reported by other workers [3,5]. The early-stage reactions are complicated by the apparent conversion of some 7 Å regions to a chloritic 14 Å structure which coexists with the 7 Å and collapsed regions to ~ 900°C. At

900–1000°C the 7 Å amesite structure dehydroxylates, with the immediate formation of a cubic spinel phase. The previously-formed collapsed phase also disappears at this stage, the final products being crystalline spinel, sapphirine and forsterite.

Amesite, with its octahedral Mg sites partly substituted by Al, is intermediate between the fully magnesian and fully aluminian 1 : 1 layer silicates serpentine and kaolinite (the analogy is not exact, however, because of the tetrahedral Al–for–Si substitution in amesite). On thermal dehydroxylation, serpentines immediately form crystalline products, probably by an inhomogeneous mechanism involving counter-migration of protons and cations through a relatively stable oxygen framework [32]. By contrast, kaolinite dehydroxylates to metakaolinite, a poorly crystalline phase which persists for several hundred degrees before forming crystalline mullite ($3\ Al_2O_3 \cdot 2\ SiO_2$) via a cubic intermediate containing both Al and Si [16]. There is some debate as to whether the oxygen structure of metakaolinite is sufficiently ordered for the reaction mechanism to be considered inhomogeneous.

The first-stage water loss in amesite somewhat resembles the kaolinite reaction, in forming a cubic close-packed intermediate phase, stable over several hundred degrees, albeit considerably better ordered than metakaolinite. In this respect, the early reaction is like that of cronstedtite [33], in which considerable structural order is maintained during the formation of an Fe–Si spinel. This could suggest that the early-stage reaction is initiated in regions of extensive iron substitution, particularly since early-stage water loss from the iron-rich A2 is greater than from A1, but the present work provides no evidence of iron segregation in these amesites. Further, although complete Fe^{2+} oxidation occurs during the early-stage reaction in air, the water formed by this redox mechanism (calculated from the iron analyses as 0.12 and 1.03% in A1 and A2, respectively) represents only a small proportion of the early-stage water loss.

The decomposition of the 7 Å amesite regions at 900–1000°C resembles the reaction of serpentine in the immediate formation of products, principally spinel, by a reaction of the type

$$9\ Mg_2Al_2SiO_5(OH)_4 \rightarrow 9\ MgAl_2O_4 + 9\ MgSiO_3 + 18\ H_2O \qquad (1)$$

This equation probably does not properly describe the reaction, since enstatite ($MgSiO_3$) is not a major reaction product. If a degree of structural continuity occurs, the spinel may inherit features of the reactant, particularly Si substitution for Mg, Al, or both. Substitution of 1 Si for 2 Mg gives the spinel $Mg_{0.75}Al_2Si_{0.125}\square_{0.125}O_4$, whereas substitution of 3 Si for 4 Al gives $MgAl_{1.5}Si_{0.375}\square_{0.125}O_4$; the formation of both these spinels by an equation analogous to (1) is accompanied by forsterite and free silica, and in the case of the latter spinel, the stoichiometry is satisfied by the additional formation of sapphirine ($Mg_{3.5}Al_9Si_{1.5}O_{20}$). Substitution of 3 Mg + 2 Al by 3 Si gives a spinel of sapphirine-like composition, which would form from amesite by a

reaction of the type

$$9\ Mg_2Al_2SiO_5(OH)_4 \rightarrow 9\ Mg_{0.625}Al_{1.75}Si_{0.375}\square_{0.25}O_4 + 1\tfrac{1}{8}\ MgAl_2O_4 + 5\tfrac{5}{8}\ Mg_2SiO_4 + 18\ H_2O \quad (2)$$

Although the detailed stoichiometry depends on reactant composition, eqn. (2) accounts for the appearance of the major observed phases without the formation of free silica. The transition from sapphirine-like spinel to true sapphirine ($Mg_{0.7}Al_{1.8}Si_{0.3}O_4$) requires only minor adjustments in cation distribution, both structures being based on cubic close-packed oxygen configurations.

The strong degree of structural continuity evident in both the early and later-stage reactions suggests inhomogeneous dehydroxylation mechanisms, but their details are complicated by the effects of lattice redox reactions and the formation and decomposition of 14 Å regions.

CONCLUSIONS

Saranovskoye and Chester amesites are both predominantly of 7 Å layer structure, but also contain X-ray reflections consistent with 14 Å regions, the intensity of which can be reduced but not entirely eliminated by thermal and acid "purification" treatments. Both amesites have virtually identical IR spectra characteristic of ordered Al-for-Si substitution, at variance with a previous suggestion that Saranovskoye amesite is disordered [19]. Iron is not present in an impurity phase, since the Mössbauer spectra are unchanged by purification treatment.

On heating in oxidising or reducing atmospheres, both amesites lose water in at least two stages, the first (at ~ 550–800°C) accompanied by the appearance of new, broad X-ray peaks consistent with regions of close-packed oxygen structure which coexist with the 7 Å amesite and 14 Å chloritic regions. During the first water loss, the typical amesite IR spectrum is retained, with broadening and loss of detail, and, in air, all ferrous iron is oxidised.

The final water loss, at 800–1000°C is accompanied by the loss of both the 7 Å amesite peaks and the transitory cubic peaks, and the appearance of new crystalline phases (spinel and sapphirine). A simple, broad IR spectrum develops, consistent with a mixture of cubic phases, but not free silica. On further heating, the crystallinity of the products improves. In air, the iron appears to be associated with the sapphirine, but in H_2/N_2, an unusual singlet Mössbauer peak occurs, which, by analogy with its occurrence in other cubic compounds, is tentatively assigned to zero-valency iron in a symmetric cubic site.

A suggestion that the spinel formed by dehydroxylation of 7 Å phase

contains silicon is consistent with the observed structural continuity of the reaction, and satisfactorily explains the formation of all the major products.

ACKNOWLEDGEMENTS

The authors are indebted to Dr. P.E. Desautels, Smithsonian Institution, Washington, for the amesite samples, Mr. A.D. Cody for the chemical analyses, Dr. L.M. Parker for the evolved gas analyses, and Dr. J.H. Johnston for the use of the Mössbauer spectrometer. Helpful discussions of the X-ray results with Dr. K.L. Brown were also appreciated.

REFERENCES

1 B.W. Nelson and R. Roy, Am. Mineral., 43 (1958) 707.
2 E.S. Dana, System of Mineralogy, Wiley, New York, 6th edn., 1903, p. 655.
3 G.W. Brindley, B.M. Oughton and R.F. Youell, Acta Crystallogr., 4 (1951) 552.
4 G.L. Taylor, A.P. Ruotsala and R.O. Keeling, Clays Clay Miner., 16 (1968) 381.
5 H. Steinfink and G. Brunton, Acta Crystallogr., 9 (1956) 487.
6 F.V. Shannon, Proc. U.S. Natl. Mus., 58 (1921) 371.
7 B.W. Nelson and R. Roy, NAS-NRC Publ., 327 (1954) 335.
8 R.C. MacKenzie (Ed.), The Differential Thermal Investigation of Clays, Min. Soc. Monograph, London, 1957, Chap. 8.
9 G.W. Brindley and F.H. Gillery, NAS-NRC Publ., 327 (1954) 349.
10 J.W. Gruner, Am. Mineral., 29 (1944) 422.
11 S.H. Hall and S.W. Bailey, Clays Clay Miner., 27 (1979) 241.
12 G.W. Brindley and G. Brown (Eds.), Crystal Structures of Clay Minerals and Their X-Ray Identification, Min. Soc. Monograph No. 5, London, 1980, Chap. 5.
13 W.A. Deer, R.A. Howie and J. Zussman, Rock Forming Minerals, Vol. 3, Longmans, London, 1962, p. 140.
14 G.M. Friedman, Am. Mineral., 37 (1952) 244.
15 N.D. Chatterjee and W. Schreyer, Contrib. Mineral. Petrol., 36 (1972) 49.
16 N.H. Brett, K.J.D. MacKenzie and J.H. Sharp, Q. Rev. Chem. Soc., 24 (1970) 185.
17 H.T. Evans, D.E. Appleman and D.S. Handwerker, Annu. Meet. Am. Cryst. Assoc., (1963) 42.
18 P.B. Moore, Am. Mineral., 54 (1969) 31.
19 C.J. Serna, B.D. Velde and J.L. White, Am. Mineral., 62 (1977) 296.
20 V.C. Farmer (Ed.), The Infrared Spectra of Minerals, Min. Soc. Monograph No. 5, London, 1974, pp. 343–348.
21 C.J. Serna, J.L. White and B.D. Velde, Mineral. Mag., 43 (1979) 141.
22 J. Preudhomme and P. Tarte, Spectrochim. Acta Part A, 27 (1971) 1817.
23 R. Jeanloz, Phys. Chem. Miner., 5 (1980) 327.
24 A.S. Povarennykh, Bull. Soc. Fr. Mineral. Cristallogr., 93 (1970) 224.
25 T. Ericsson, R. Wappling and K. Punakivi, Geol. Foeren. Stockholm Foerh., 99 (1977) 229.
26 I. Rozenson, E.R. Bauminger and L. Heller-Kallai, Am. Mineral., 64 (1979) 893.
27 C. Blaauw, G. Stroink, W. Leiper and M. Zentilli, Can. Mineral., 17 (1979) 713.
28 T.V. Malysheva, L.M. Satarova and N.P. Polyakova, Geochem. Int., 14 (1977) 117.

29 G.M. Bancroft, R.G. Burns and A.J. Stone, Geochim. Cosmochim. Acta, 32 (1968) 547.
30 K.J.D. MacKenzie, J. Mater. Sci., 17 (1982) 1834.
31 H.R. Leider and D.N. Pipkorn, Phys. Rev., 165 (1968) 494.
32 G.W. Brindley and R. Hayami, Mineral. Mag., 35 (1965) 189.
33 K.J.D. MacKenzie and R.M. Berezowski, Thermochim. Acta, 44 (1981) 171.